



Título artículo / Títol article:

Unraveling Reaction Mechanisms by Means of Quantum Chemical Topology Analysis

Autores / Autors

ANDRÉS, Juan; GONZÁLEZ-NAVARRETE, Patricio; SAFONT, Vicent Sixte

Revista:

International Journal of Quantum Chemistry

Versión / Versió:

Postprint

Cita bibliográfica / Cita bibliogràfica (ISO 690):

ANDRÉS, Juan; GONZÁLEZ-NAVARRETE, Patricio; SAFONT, Vicent Sixte. Unraveling reaction mechanisms by means of Quantum Chemical Topology Analysis. *International Journal of Quantum Chemistry*, 2014, vol. 114, no 19, p. 1239-1252.

url Repositori UJI:

<http://hdl.handle.net/10234/135065>

Unraveling Reaction Mechanisms by means of Quantum Chemical Topology Analysis

Juan Andrés*, Patricio González-Navarrete, and Vicent Sixte Safont

Departament de Química Física i Analítica, Universitat Jaume I, 12071 Castelló, Spain

*Corresponding author: andres@qfa.uji.es

Abstract

A chemical reaction can be understood in terms of geometrical changes of the molecular structures and reordering of the electronic densities involved in the process; therefore, identifying structural and electronic density changes taking place along the reaction coordinate renders valuable information on reaction mechanism. Understanding the atomic rearrangements that occur during chemical reactions is of great importance and this perspective aims to highlight the major developments in quantum chemical topology analysis, based on the combination of electron localization function and catastrophe theory as useful tools in elucidating the bonding and reactivity patterns of molecules. It reveals all the expected, but still ambiguous, elements of electronic structure extensively used by chemists.

The chemical bonds determine chemical reactivity and this technique offers the possibility of their visualization, allowing chemists to understand how atoms bond, how and where bonds are broken/formed along a given reaction pathway at a most fundamental level, and so, better following and understanding the changes in the bond pattern. Their results clearly herald a new era, in which the atomic imaging of chemical bonds will constitute a new method for examining chemical structures and reaction mechanisms. The important feature of this procedure is that in practice the scope of its values is system-independent. In addition, from a practical point of view, it is cheap to calculate and implement because wave functions are the required input, which are easily available from standard calculations. To capture these results two reaction mechanisms: isomerization of $C(BH)_2$ carbene and the thermal cycloheptatriene-norcaradiene isomerizations have been selected, indicating both the generality and utility of this type of analysis.

1. Introduction

“Sometimes it seems to me that a bond between two atoms has become so real, so tangible, so friendly, that I can almost see it. Then I awake with a little shock, for a chemical bond is not a real thing. It does not exist. No one has ever seen one. No one ever can. It is a figment of our own imagination.”

Charles A. Coulson *The Spirit of Applied Mathematics* 20–21 (Clarendon Press, 1953)

In the study of science, understanding the concepts, models and theories is fundamental, playing an important role when scientific knowledge is developed and when science is communicated. Concepts can be described as entities of which the world is believed to consist of; models, as proposals for how these concepts physically and temporarily correlate to each other in the material world; and theories, as general sets of reasons why these concepts and models can be thought to occur^[1-3]. In this sense, it is important to remark that no chemical education would be possible and no scientific progress would have been achieved without strong concepts. However, there is an absence of physically rigorous definitions for some concepts that a chemist uses in his everyday work as fundamental as atomic and molecular orbitals, atomic charges, nucleophilic or electrophilic character, electron pair, or even covalent or ionic bonds. They do not correspond to physical observables. Such concepts therefore cannot be unambiguously defined in pure quantum theory. In particular, chemical bonds and their reorganization are central concepts in chemistry and they are at the heart of understanding the chemical structure and reactivity, respectively. Despite its importance, a precise and unambiguous definition of when a chemical bond exists between (usually two) atoms and its nature continues to be debated.^[4-6]

The concept of chemical bond is supported by a multiplicity of criteria derived from experimental measurements, such as distances, energies, force constants, spectroscopic and magnetic properties, as well as theoretical ones and this situation leads to a wide range of loosely related concepts and parameters. As pointed out by Alvarez et al.^[7]: “If one allows oneself to use a multiplicity of criteria, bonds may exist by one measure, not by another. This is not a reason touring our hands, nor complaining how unscientific chemistry is (or how obstinate chemists are). Chemistry has done more than well in creating a universe of structure and function on the molecular level with just this imperfectly defined concept of a chemical bond. Or maybe it has done so well precisely because the concept is flexible and fuzzy”. Therefore, chemical bond is the

archetypal example of a fuzzy concept, as many others in chemistry^[6,8]. In this respect, chemical bonds have been compared to unicorns: mythical creatures that everyone knows how they look, despite nobody ever having seen one,^[9-11] or they have even been decribed as “noumenon” rather than as “phenomenon”.^[5,12,13]

Although the methods and techniques of the theoretical and computational chemistry have advanced extraordinarily in recent years, the theoretical definition of chemical bond is still problematic. Even in a very recent paper by Backsay and Nordholm, this matter of how to define a covalent bond has been discussed.^[14] These authors point out that there are two different schools of thought concerning the mechanism of covalent bonding and the difference lies in the different methods of analyzing quantum mechanical results. According to Hellmann, Ruedenberg and Kutzelnigg, a lowering of the kinetic energy associated with electron delocalization is the key stabilization mechanism. And in broad agreement with Ruedenberg’s ideas, Esterhuysen and Frenking^[15] have proposed an energy decomposition analysis that highlights the importance of electrostatic and Pauli repulsion effects in a range of covalently bound molecules. In contrast, the opposing view of Slater, Feynman and Bader has maintained that the source of stabilization is electrostatic potential energy lowering due to electron density redistribution to binding regions between nuclei. As it was remarked by Adamo et al.^[16]: “Although all chemical information is in principle included in the Schrödinger equation and in the derived electron density (and wave function), chemists however still aim to develop interpretative tools that, even if they may contain less information, are very useful to straightforwardly account for (or even predict) a certain number of relevant physicochemical properties. These tools can be either rooted in a mere pragmatic approach or in more fundamental theories. There is nevertheless no reason that these two frameworks should be separate”.

2. Reaction Mechanism

Chemical reactions, in general, manifest essentially rearrangements of the nuclei, which are directly related to the forming/breaking bond processes along the reaction and therefore, understanding a chemical process requires basically or fundamentally the knowledge of its molecular mechanism. For its part, the reaction mechanism corresponds to the mapping of the atoms from reactants to products, identifying not only the nature of the changing atoms but also the sequence of breaking

and forming of the bonds between them. This is one of the “Holy Grails”, dream and challenge of chemistry for a long time: to directly “watch” chemical reactions at the atomic scale, i.e. when and how the bond breaking/forming processes occur along a given reaction pathway. Therefore, we need quantitative descriptions of the corresponding reaction mechanisms.

In chemical reactivity, a reaction mechanism represents a sequence of elementary steps by which overall chemical change occurs, describing in detail what is taking place at each stage of a chemical transformation, i.e. the way in which chemical events such as chemical bonds that are broken/formed, electron pair rearrangements, transformation of formally double to simple bonds or *viceversa*, etc. This concept is essential in chemical education as a fundamental tool enabling the comprehensive representation of the reaction mechanism associated with a chemical reaction. In this sense, an elementary reaction can be related to a single electron movement (e.g., radical reactions), movement of a single pair of electrons (e.g., simple addition or bond dissociation reactions), or the complex concerted movement of many electrons [e.g., substitution (S_N2), pericyclic or second-order elimination (E2) reactions].

In chemistry textbooks, these processes are still imagined and subsequently represented by drawings or models using curly arrows. In general, the tails and heads of the curly arrows indicate chemical bonds that are weakened and strengthened due to loss or gain of valence electron density during the reaction, respectively. Mechanistic reactions can be drawn as “arrow-pushing” diagrams^[17] showing the concerted electron movements. This representation appears to be a consequence of the chemical intuition and is a fundamental part of the chemist’s activity, although there is no experimental support for these curly arrows. Many examples can be found in textbooks of organic chemistry^[17-23], inorganic chemistry,^[24,25] and biochemistry.^[26,27] Therefore, organic and inorganic chemists, as well as biochemists, have developed and applied powerful albeit less quantitative rules for electronic redistributions which accompany the nuclear motions along the course of a given chemical rearrangement. Even in recent years, bond arrows “ \rightarrow ” have been used to describe structures involving main-group compounds^[28].

In a very recent essay entitled: “Chemistry: A Panoply of Arrows”, Prof. Álvarez^[29] presented an overview on the historical use of arrows in chemistry, providing the variety of meanings that a simple symbol such as an arrow may have: the alchemical symbols representing elements or compounds; in chemical equations to show the reversibility of a given chemical process; double-headed arrow to represent

resonance structures or even tautomerism associated with the interconversion of two isomers through a simultaneous shift of a double bond and a proton; in orbital energy diagrams; in the Jablonski diagrams indicating radiative (straight arrows) and nonradiative (wavy arrows) transitions; in the stimulated emission of radiation that takes place in lasers; and up- and down-pointing arrows to depict the positive- and negative spin of an electron.

In the context of quantum mechanics, a molecular process is described completely by the time-dependent state vector $|\Psi(t)\rangle$, which evolves according to Schrödinger's equation governing the simultaneous coupled motions of electrons and nuclei. In the most common instance, the process is taken to be electronically adiabatic (i.e., the light, fast electrons adjust instantaneously to the movements of the heavy, slow nuclei). To describe such process, one typically invokes the Born-Oppenheimer approximation (BOA).^[30-32] From this approximation, the concept of potential energy surface (PES) is derived, playing a central role in the theory and computational simulation of chemical structure and reactivity. Particular interest has been focused on extracting information from the stationary points of the energy surface. In the BOA framework, minima on the N -dimensional PES for the nuclei can be identified with the classical picture of equilibrium structures of molecules and saddle points can be related to transition states (TSs) and reaction rates. Within this approach, minima and saddle points have been fully characterized through the first and second derivatives of the energy (gradient and Hessian) over the nuclei positions. The reaction mechanisms can therefore be modelled as minimum energy paths between stable configurations on a high-dimensional PES, where saddle points represent transition and minima are associated with reactants, products and possible intermediates.^[33] In this context, PESs are almost always system-specific and must be obtained from quantum mechanical electronic structure calculations.

3. Electron density $\rho(\mathbf{r})$

The simple reason of why the definition of chemical bond is difficult is that electronic bonding interactions are not directly observable as Coulson asserts,^[34] i.e. no quantum mechanical "chemical bond operator" exists that would provide the desired answer, for example, as a conventional expectation value. As Fleming Crim of the University of Wisconsin–Madison puts it, cited by P. Ball^[8]: "A bond is an entity described by

quantum mechanics but not a fixed ‘entity’ in that it will behave differently depending on how we perturb and interrogate it”, but our intuitive perception of molecular phenomena in the three-dimensional space demands such representation. Thus, interpretative tools are necessary to recover chemical structure and reactivity and more specifically to understand the process of bond formation and breaking during reactions. With a similar perspective, Lewis conceived the idea of electron pairs.^[35] The description of electron pairs is at the heart of understanding the chemistry of a given compound because reorganization of electron pairs drives any chemical reaction and it is based on the seminal work of Lewis, identifying chemical bonds with electron pairs shared between the bonded atoms.^[36]

The basic assumption is that the existence of a chemical bond must be related to some observable, a measurable property of the system, and demands a three-dimensional space representation. In order to overcome these difficulties and to dispose of a general method of interpretation, a mathematical model of the chemical description of the matter is necessary, consistent with the postulates of quantum mechanics, valid for exact wave functions and therefore, independent of the way of calculation. This mathematical model is not unique because different spaces (geometrical direct space, momentum space, Hilbert space) as well as different mathematical theories external to Quantum Mechanics can be used for this purpose. As remarked by Daudel et al.: “Theories derived accordingly should provide the mathematical bridge between the chemical intuition and wave mechanics, which may be considered as a theoretical justification of the main chemical ideas.”^[37]

It is well known that the electron density is of paramount importance to fully understand the ground state properties of many-electron systems. As remarked by Yang et al.^[38]: “Interactions between electrons determine the structure and properties of matter from molecules to solids. To describe interacting electrons, the extremely simple three-dimensional electron density can be used as the basic variable within density functional theory (DFT),^[39,40] negating the need in many cases for the massively complex many-dimensional wave function”. Its prominence derives from the Hohenberg-Kohn theorem (HKT),^[41] which has shown the existence of a functional relation between the ground state electron distribution and the ground state wave function of electronic systems. However, in 1963, a year before the historical discovery of the foundations of modern DFT, Bader and Jones wrote:^[42] “The manner in which the electron density is disposed

in a molecule has not received the attention its importance would seem to merit". Unlike the energy of a molecular system which requires a knowledge of the second-order density matrix for its evaluation,^[43] many of the observable properties of a molecule are determined in whole or in part by the simple three-dimensional electron-density distribution.

As mentioned, chemical bonds are not direct observables. However, an adequate representation as well as the description of the bond breaking/forming processes should be provided by a physical observable defined in the coordinate space. The electron density, $\rho(r)$, meets these requirements because it is an experimental accessible scalar field, which is a local function defined within the exact many-body theory, supported by the HKT. The importance of $\rho(r)$ as a fundamental property of an electronic system is highlighted by HKT. It states that the ground-state energy of a non-degenerate quantum chemical system is functionally related to its distribution of charge. $\rho(r)$ is a fundamental Dirac observable that completely defines the ground state of an electronic system.^[41] In this regard, an experimentally or theoretically determined charge density yields a wealth of information about the electronic structure of atoms, molecules and solids.^[44,45]

4. Quantum Chemical Topology

As mentioned by Bader^[46]: "Dirac defines an observable to be a linear Hermitian operator expressible in terms of the dynamical (position and momentum) variables with a complete set of eigenfunctions, the base states that are employed in the representation of the state vector", a definition prompting the usage 'Dirac observable'.^[47] A change in representation of the state vector from one set of base states that are eigenfunctions of one particular set of commuting observables to another, is accomplished using Dirac's transformation theory. There is a Dirac observable associated with every property and it acts on a state vector to yield eigenvalues or expectation values that may or may not be measurable. Each observable obeys a Heisenberg equation of motion and these equations yield the theorems of quantum mechanics; examples being the virial theorem and the Ehrenfest and Feynman force theorems. Through these theorems, one is able to predict and understand the properties of a system and relate the values of the observables to the forces that define the system.

To adequately describe these properties of chemical reacting systems, additional tools for extracting observable information are necessary. Bader's quantum theory of atoms in molecules (QTAIM) is nowadays often invoked to analyze the electron density, to describe interatomic interactions and to rationalize chemical bonding properties as true observables of the electron wave function^[48-55]. QTAIM works by proving that the topological condition of zero-flux ($\Delta\rho(\mathbf{r}) \cdot \mathbf{n}(\mathbf{r}) = 0$) of the charge density $\rho(\mathbf{r})$ serves as the boundary condition for the application of Schwinger's principle of stationary action in the definition of an open system. This method divides the three-dimensional space occupied by a molecule, into sub-elements associated with the atoms in the molecule (called atomic basins), using the electron density, $\rho(\mathbf{r})$, as the scalar function. It is mainly based on the topological analysis of $\rho(\mathbf{r})$, particularly the characterization of its critical points and the integration of every kind of quantum observable within the attraction basin of atomic nuclei.

According to the QTAIM, "the quantum mechanics of proper open systems yields the physics that governs the local behavior of $\rho(\mathbf{r})$ ". All bond paths, lines of maximum density linking neighboring nuclei in a system in stable electrostatic equilibrium, have a common physical origin. The presence of a bond path and its associated virial path provide a universal indicator of bonding between the atoms so linked.^[56] Moreover, the topology of the charge density, $\rho(\mathbf{r})$, allows one to define bond paths and critical points (where $\nabla\rho = 0$). The Laplacian of $\rho(\mathbf{r})$, $\nabla^2\rho(\mathbf{r})$, at the critical point measures to what extent the electron density is locally concentrated if $\nabla^2\rho(\mathbf{r}) > 0$ (associated with closed-shell interactions, such as ionic bonds, hydrogen bonds, and van der Waals molecules, etc.), or depleted if $\nabla^2\rho(\mathbf{r}) < 0$ (associated with shared interactions, such as dative or covalent bonds). For a concise summary of the QTAIM classification of bonding interactions, see Bianchi et al^[57] and Matta.^[58]

One of the goals of the topological analysis of electron distribution functions is to provide a partition of the geometrical space occupied by the chemical system of interest (molecule, aggregate, polymer, 1-3D periodic system) into adjacent non-overlapping volumes called basins. These basins are thought to correspond to chemical entities such as atoms in molecules, atomic cores, bonds or lone pairs. The partition is achieved with the help of a rigorous mathematical method, namely the Dynamical System Theory,^[59,60] applied to the gradient vector field of a quantum mechanically

defined local function of the electron distribution which carries the chemical information.

The relationship between charge density topology and physical/chemical properties can be understood from HKT as it asserts that a system's ground-state properties are a consequence of its charge density.^[41] Since chemical reactions proceed by $\rho(r)$ redistributions, the methods that deal with the analysis of the $\rho(r)$ distribution should have a particular appeal for chemists and help to understand the electron structure of molecules and thus, chemical reactivity.^[48] In addition, these methods are not only useful for quantum chemical calculations but also for analyzing experimentally determined electron densities.^[61]

QTAIM has inspired topological analysis of functions other than the electron density. The most popular alternative partition of the molecular space is provided by the topological analysis of the electron localization function (ELF), originally introduced by Becke and Edgecombe,^[62-64] that is derived from the consideration of an approximate conditional pair density. And similarly to the Bader's topological analysis of the electron density, the ELF values can also be treated as a continuous and differentiable scalar field in 3D space. The function not only contains information on the structure of atomic shells but also clearly displays the location and size of bonding and lone electron pairs.^[65,66] ELF can be understood, in words of D. B. Chesnut, as "a local measure of the Pauli repulsion between electrons due to the exclusion principle" that "allows one to define regions of space that are associated with different electron pairs in a molecule".^[67] In this context, and very recently, Gadre et al.^[68] have addressed questions such as: can a lone pair be defined in terms of physical observables? How can the properties of a lone pair be described?

Popelier proposed that these type of studies form a unified theoretical framework, named Quantum Chemical Topology (QCT) inspired in the seminal work of Bader,^[48,49,51,69-71] for general topological analysis of scalar functions, such as the source function,^[72] the momentum density,^[73] the electron pair density,^[74] the nuclear potential energy field,^[75] the virial field,^[76] as well as the Laplacian of charge density.^[48,53,77,78] In fact, topological analysis of various scalar fields, different to electron density, is now used in computational chemistry, such as the scalar field derived from the molecular electrostatic potential^[79]; even the mathematical framework of topological analysis has been applied by Mezey on the study of potential energy hypersurfaces.^[80,81]

Chemical reactions are always associated with electronic density changes of the involved chemical species. Determining the electronic density of all atoms can lead to an understanding of the reaction pathways. However, often the reactions are too complex and too fast to be measured at *in situ* conditions due to slow and/or insensitive experimental techniques. One step further is based on the idea that it is reasonable to think that an adequate representation of these chemical events should be given by a physical observable defined in coordinate space. The electron density is the best choice because it is a local function defined within the exact many body theory, and it is also an experimentally accessible scalar field. Its paramount role in the description of many-body problems is supported by HKT.^[41] The DFT^[39,41] asserts that the single particle density $\rho(\mathbf{r})$ contains all the information of a system and the total energy attains the minimum value for the true density.

This perspective presents a personal overview of the current status of the quantum chemical topology analysis applied to chemical reactivity. We attempt to assess the status of the field for two reactions: the simple isomerization of carbene $\text{C}(\text{BH})_2$ and a complex process corresponding to the thermal norcaradiene-cycloheptatriene isomerization, in order to point out both the generality and utility of the analysis of reaction mechanism. We hope this perspective will be useful to highlight recent advances and to identify important areas for future research.

5. The Bonding Evolution Theory

The analysis of the electronic structure at the stationary points (reactants, products, possible intermediates and transition structures, TSs) is one of the most relevant applications of modern computational chemistry. However, the calculations of accurate data for the geometries, energies and other observable properties are not always guaranteed. In contrast, very important part of quantum chemical research has been devoted to interpret the results in terms of quantitative concepts derived from first principle calculations. The current electronic structure theory of molecules can actually provide the accurate snapshots of electronic distribution associated with geometrical changes of very large molecules. Although HKT guarantees that all the molecular information is encoded in the electron density, the physical description of chemical systems requires additional postulates for extracting observable information in terms of atomic contributions. This is achieved by the QTAIM introduced by Bader,^[48] as

explained before. The proper open system concept provides a quantum topological partitioning of the molecular space into chemically transferable molecular fragments for which the energy and all other measurable properties can be precisely defined.^[82] Thus, the introduction of concepts such as bond path in the framework of QTAIM^[56] has allowed the description of the evolution of the electronic structure along a reaction path. In this sense, a molecular mechanism of a given chemical reaction can be studied from the redistribution of the electron density along the reaction path connecting the stationary points. Bader and co-workers pioneered the study of the structural change based on the electron density using Thom's theory of elementary catastrophes (CT).^[83] The reader can refer to the Bader's milestone book.^[48] The mathematical foundations as well as the available computational results were reviewed comprehensively.^[84,86-88]

However, the applicability of QTAIM to the study of reaction mechanisms rapidly appeared to be mostly limited to intramolecular processes because there is no topological change in the charge density gradient field when a diatom dissociates. Bader's methodology has been further revised by Krokidis et al.^[89] who used the ELF instead of the charge density. Thus, the topological analysis of the ELF^[62,63,90] is becoming increasingly popular in the characterization of chemical bonding in systems ranging from clusters in the gas phase to solids. In this sense, Silvi and co-workers have developed the Bonding Evolution Theory (BET) as a generalization of Bader's work and to other scalar fields as ELF.^[89,91]

The topological partition of the ELF gradient field yields basins of attractors, which can be thought as chemical local objects such as atomic cores, bonds and lone pairs. These basins are either core basins labeled $C(A)$ or valence basins $V(A, \dots)$, where A is the atomic symbol of the element. The valence basins are characterized by their coordination number, that is equal to the number of neighboring core basins. This number is called synaptic order.^[92] In addition, changes in the control parameters defining the reaction pathway (such as the nuclear coordinates and the electronic state) can lead to different topologies of the ELF. According to the theory of dynamics systems, a system can be considered structurally stable if a small perturbation is only possible for values of the control parameters comprised into well-defined ranges, namely structural stability domains (SSDs), where all the critical points are hyperbolic and separated by catastrophic points in which at least one critical point is non-hyperbolic. Along the reaction pathway the chemical system goes from a given ELF-

SSD to another by means of bifurcation catastrophes occurring at the turning points. The bifurcation catastrophes occurring at these turning points are identified according to Thom's classification.^[83]

Indeed, a chemical reaction can be viewed as a sequence of elementary chemical processes characterized by a catastrophe. Only three types of bifurcation catastrophes have been found in chemical reactivity: (i) the fold catastrophe, corresponding to the creation or annihilation of two critical points of different parity; (ii) the cusp catastrophe, which transforms one critical point into three (and *viceversa*) such as in the formation or the breaking of a covalent bond; (iii) the elliptic umbilic, in which the index of a critical point changes by two. The identification of the turning points connecting the ELF-SSDs along the reaction pathway allows a rigorous characterization of the sequence of electron pair rearrangements taking place during a chemical transformation, such as multiple bond forming/breaking processes, creation/annihilation of lone pairs, transformations of double bonds into single ones or vice versa, and other electronic rearrangements. The sequence of catastrophes that takes place along the reaction pathway can be represented by the general formula introduced by Berski et al.^[93]

$$N_1-N_2-FCSHEBP-N_3$$

where N_1 is the ordinal number of analyzed sequence which can be omitted only when one reaction is considered, i.e. $N_1=1$. The number of SSDs is represented by N_2 . *FCSHEBP* are the symbols of the catastrophes according to Thom's classification, i.e. *F* = fold, *C* = cusp, *S* = swallow tail, *H* = hyperbolic umbilic, *E* = elliptic umbilic, *B* = butterfly and *P* = parabolic umbilic. N_3 represents the end of the sequence ($N_3=0$). In addition, the † superscript is utilized in those catastrophes where either the number of attractors or the synaptic order increase, e.g. F^\dagger corresponds to a fold type catastrophe in which a new attractor is created. The symbol of catastrophe written in bold is used to mark a catastrophe leading to formation of first covalent bond (for example, ***F***).

6. Working examples

As stated before, a molecular mechanism of a given chemical reaction can be studied from the redistribution of the electron density along the reaction path connecting the stationary points. In the examples herein reported, we have performed the

topological analysis of the ELF, by means of TopMod package^[94], considering a cubical grid of stepsize smaller than 0.05 bohr. Starting from the TS, the reaction path has been traced following the intrinsic reaction coordinate (IRC)^[95,96], using a Rx in mass-weighted step of 0.05amu^{1/2} bohr until reaching the minimum. For each point along the IRC path, the wave function has been obtained and the ELF analysis has been performed. Other research groups have used the electron density^[97-100], its Laplacian,^[101] ELF^[93,102-107] and electrostatic potential^[79,108] to study molecular mechanisms or conformational changes of several systems using these approaches.

The first example we are going to describe in the present work is the C(BH)₂ isomerization between the bent and the linear forms of the molecule. The two isomers are nearly degenerate, as it was stated by Frenking et al. in a very recent work^[109]: definitive computations on these species with high-level theoretical treatments render that the difference in energy between the two isomers is near zero and that the activation barrier for the interconversion is around 2 kcal/mol. In this process, no forming and breaking of chemical bonds occur, although the delineation of factors that control the pair electron reorganization in this carbene on this isomerization is complicated.

Calculations at MP2/cc-pVDZ level of theory have been performed using Gaussian 09^[110] and we have found the linear isomer to be more stable than the bent one by 0.47 kcal/mol, the barrier height value being 2.75 kcal/mol. The bent isomer displays a B-C-B bond angle of 91.14 degrees, in close agreement with the value reported by Frenking et al.^[109] (90.36 degrees) at their highest theoretical level used, namely c-CCSDT(Q)/cc-pCVQZ(AE).

The energy profile along the IRC path is reported in Figure 1 together with the six SSDs found. Snapshots of the ELF basins for some selected points along the IRC, representative of the different SSDs found, are depicted in Figure 2, while the evolution of some basin populations along the IRC path is reported in Figure 3.

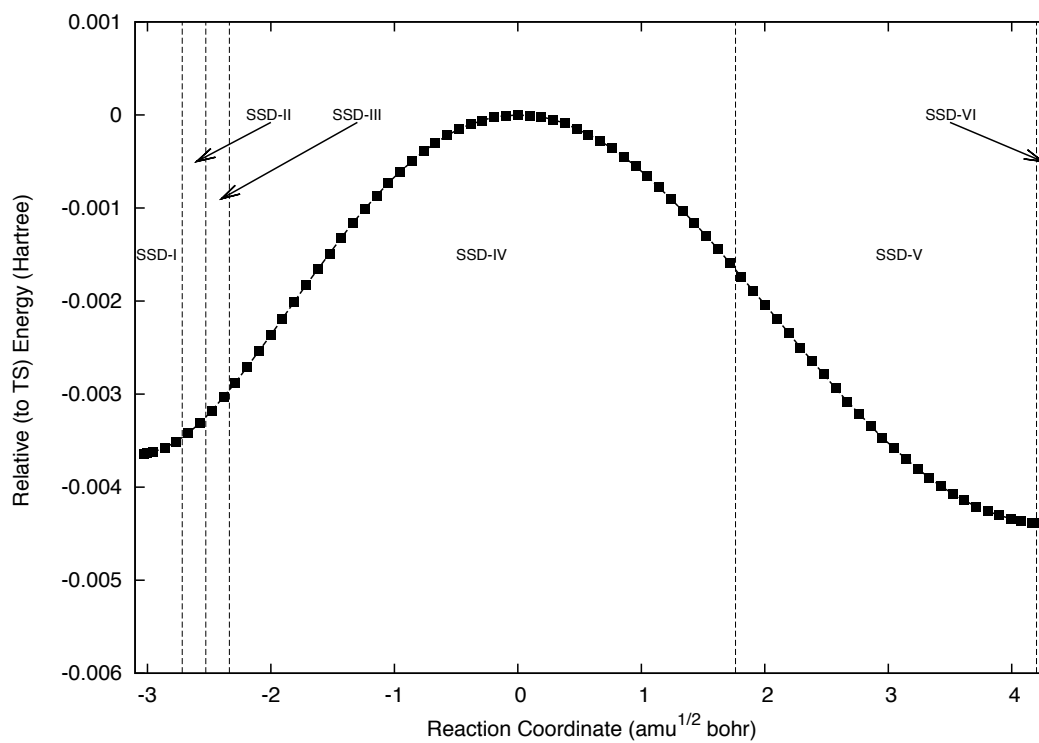


Figure 1. Energy profile for the bent (left side) to linear (right side) isomerization of $C(BH)_2$, calculated by means of the IRC method. The six domains of structural stability found are marked.

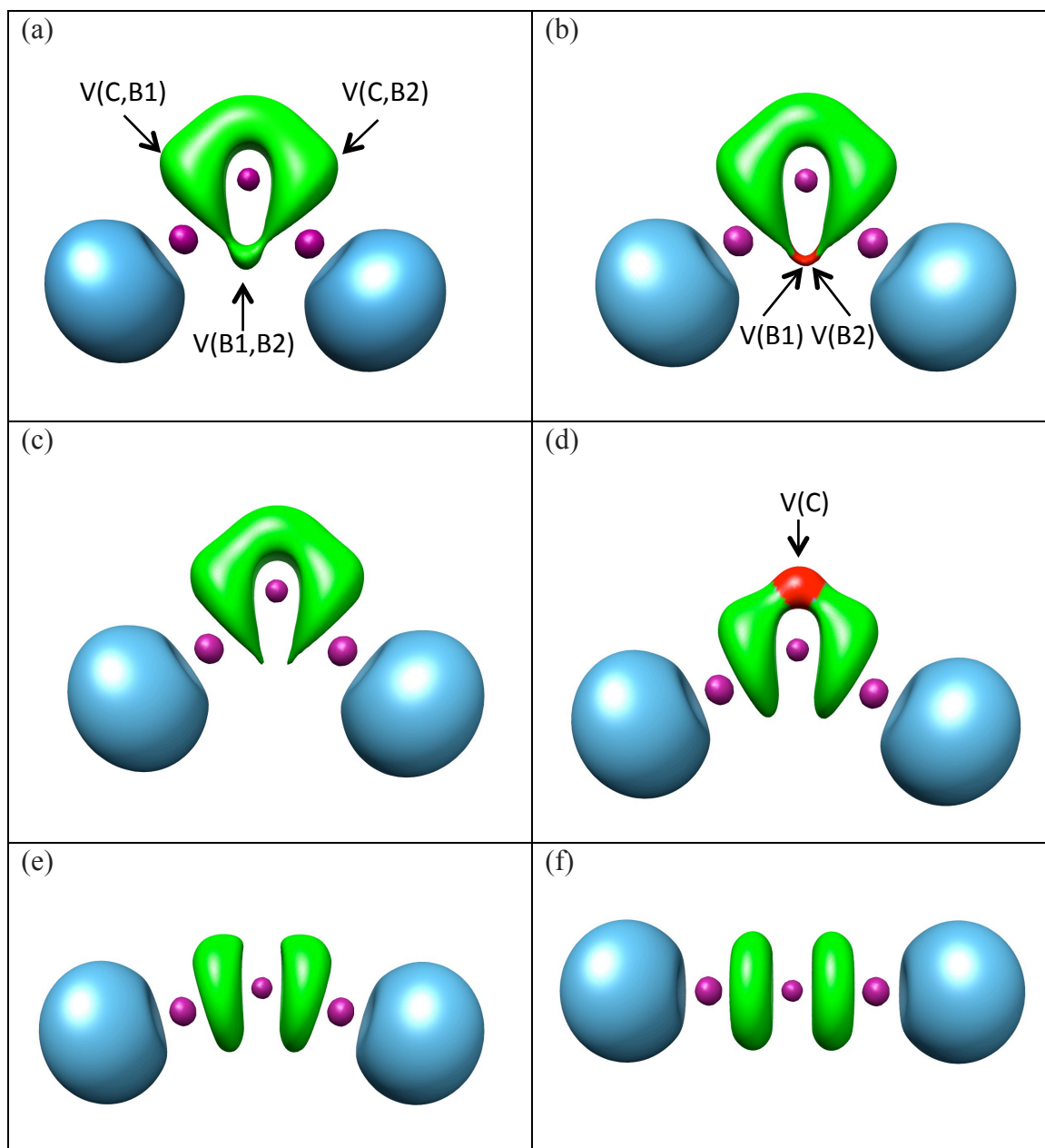


Figure 2. Snapshots of the ELF localization domains ($\eta=0.788$ isosurface) for selected points along the IRC: (a) $C(BH)_2$ bent isomer (SSD-I), (b) point at $s = -2.575 \text{ amu}^{1/2}\text{bohr}$ belonging to SSD-II, (c) point at $s = -2.384 \text{ amu}^{1/2}\text{bohr}$ belonging to SSD-III, (d) TS, belonging to SSD-IV, (e) point at $s = 1.811 \text{ amu}^{1/2}\text{bohr}$ belonging to SSD-V, (f) $C(BH)_2$ linear isomer. The color code is as follows: green, disynaptic basins; red, monosynaptic basins; blue, hydrogenated basins; purple, core basins. Names of some basins are included.

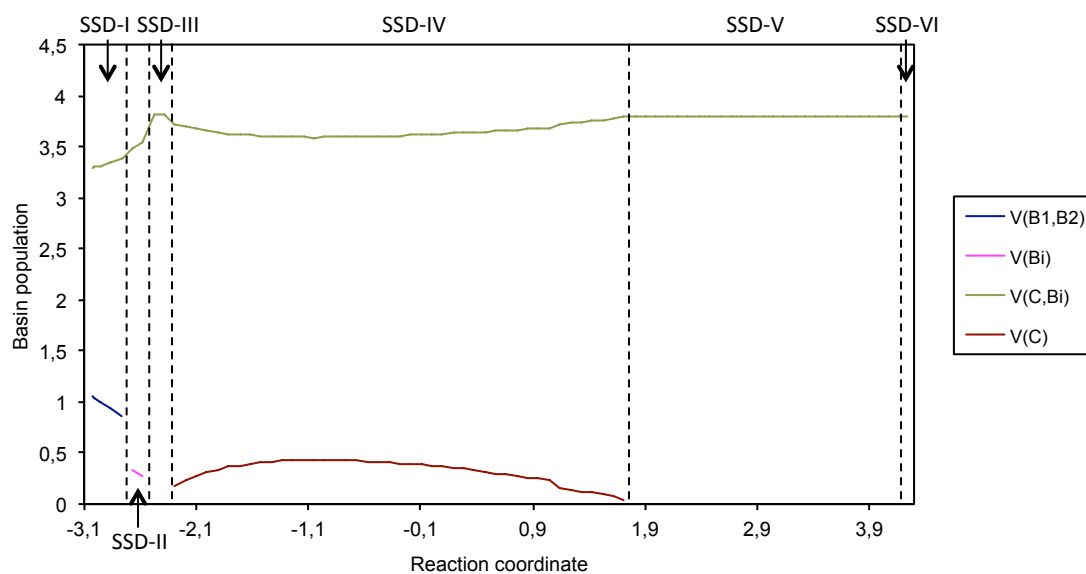
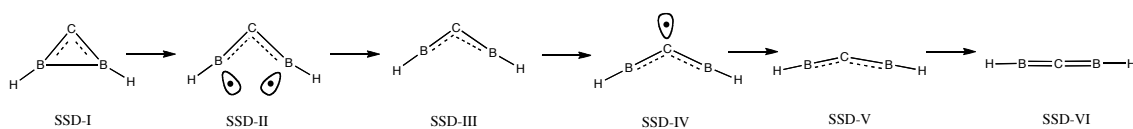


Figure 3. Population evolution of some basins along the IRC path. $V(B_i)$ stands for $V(B1)$ or $V(B2)$, and $V(C,B_i)$ stands for $V(C,B1)$ or $V(C,B2)$. Dashed lines separate the structural stability domains found, which are indicated.

The six SSDs found can be viewed as a sequence of chemical events taking place in the $C(BH)_2$ isomerization. At the bent isomer, left side of the energy profile in Figure 1, eight basins can be found, corresponding to three core basins, two hydrogenated basins and three disynaptic basins accounting for the C-B bonds and for a B-B bonding interaction. The $V(B1,B2)$ disynaptic basin population is calculated to be 1.05e electrons at this point, while the $V(C,B1)$ and $V(C,B2)$ disynaptic population basins at the bent isomer have 3.29e each. Hence, as proposed by Frenking et al.,^[109] the bent isomer can be described as a carbene (with some three center CB_2 bonding) and a little carbene character.

As it can be seen in Figure 3, the $V(B1,B2)$ population diminishes while the $V(C,B1)$ and $V(C,B2)$ populations grow accordingly along SSD-I, which reflects the gradual loss of the B1-B2 interaction and the strengthening of the C-B bond interactions. This can be better observed with the help of Scheme 1, depicted from the perspective of the ELF analysis, in which full lines and ellipses represent disynaptic and monosynaptic basins, respectively, while dotted lines indicate a large basin population.



Scheme 1. Representation of the bent-to-linear isomerization of $C(BH)_2$ from the ELF perspective.

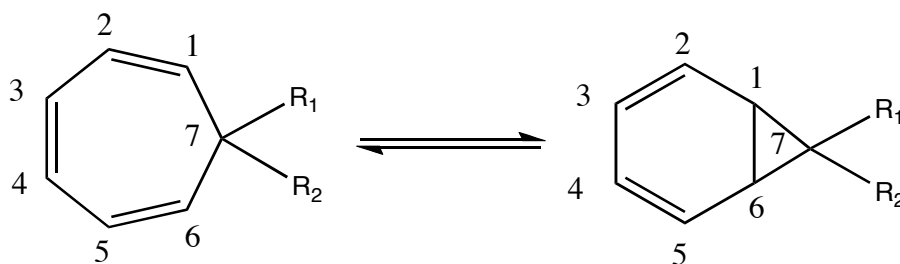
A first catastrophe (fold-type) is found at $s \approx -2.72 \text{ amu}^{1/2} \text{ bohr}$: the disynaptic basin $V(B_1, B_2)$ is split into two monosynaptic basins, with populations of $0.325e$ in the first point of the SSD-II. Meanwhile, the population of the $V(C, B_1)$ and $V(C, B_2)$ basins increases to $3.55e$.

The two monosynaptic basins $V(B)$ surrounding the boron atoms disappear when the system reaches the SSD-III, at $s \approx -2.53 \text{ amu}^{1/2} \text{ bohr}$ by means of two simultaneous fold type catastrophes, whereas the population of the $V(C, B)$ basins increases further to $3.815e$. However, almost immediately, at $s \approx -2.34 \text{ amu}^{1/2} \text{ bohr}$, a fold type catastrophe takes place and the SSD-IV is reached. A new monosynaptic basin located on the C atom appears, whose population is detracted from the two $V(C, B)$ basins, see Figure 3. The population of the new $V(C)$ basin ranges from $0.17e$ at the beginning of SSD-IV to $0.44e$ at $s = -0.954 \text{ amu}^{1/2} \text{ bohr}$, then to $0.38e$ at the TS and continues to diminish until a final value of $0.03e$ is found at the last point of SSD-IV. This domain is the largest along the IRC and it demands the highest energetic cost of the activation energy. According to the ELF topological analysis the B-B bond breaks at an early stage of the mechanism. The $V(B_1, B_2)$ basin population is calculated to be $1.05e$ for the bent isomer at the beginning of the reaction, as mentioned, indicating a weak interaction between boron atoms. A low charge density between them, therefore, promotes an early B-B breaking. In addition, while boron valence basin populations ($V(B_1, B_2)$ and subsequently $V(B)$) decrease as the reaction proceeds, the $V(C, B_i)$ basin populations increase their values until the $V(C)$ monosynaptic basin suddenly appears (see Figure 3). Note that when the $V(C)$ basin population increases, the $V(C, B_i)$ populations slightly decrease and vice versa. As a consequence, the electronic density flows toward the carbon valence shell because the isomer is not linear enough to avoid the electronic repulsion in the zone of the C-B bonds. In this sense, the SSD-IV can be thought as an intermediate stage of the reaction where an internal electronic flux takes place in order to prepare the system for the imminent formation of C-B double bonds. Therefore, a large SSD-IV is expected because of the early B1-B2 bond breaking and

the late formation of the C-B double bonds, while the transition state structure is not assumed to be part of the breaking/forming process.

At $s \approx 1.77 \text{ amu}^{1/2} \text{ bohr}$ another turning point can be found, the monosynaptic basin on C atom disappears by means of a fold type catastrophe and the SSD-V begins. At the first point inside the SSD-V, the population of the V(C,B) basins are predicted to be 3.805e. Finally, at $s \approx 4.20 \text{ amu}^{1/2} \text{ bohr}$, the last turning point is found and the SSD-VI is reached. In this domain, consisting of only one point in the IRC that corresponds to the linear isomer, the V(C,B) basins are split into two basins each, with overall populations of 3.8e, becoming apparent the coexistence of σ and π interactions between the C atom and the boron atoms due to the multiple character of the C-B bonds. As it can be seen, the ELF analysis renders that the linear $\text{C}(\text{BH})_2$ can be described as a classical cumulene, in agreement with the recent work by Frenking et al.^[109]

The second example accounts for the cycloheptatriene-norcaradiene (CHT-NCD) isomerization, which has attracted much attention for more than 40 years.^[111,112] This equilibrium (Scheme 2) includes a valence bond isomerization and a thermally allowed disrotatory electrocyclic cyclopropane ring opening. This isomerization corresponds to a complex and coupled forming and breaking of chemical bonds and, as it is shown in Scheme 2: the net structural outcome is the breaking/forming of the C1–C6 bond and the transformations of formal single C1–C2, C3–C4 and C5–C6 bonds into double ones, while an opposite behavior takes place in the C2–C3 and C4–C5 bonds.

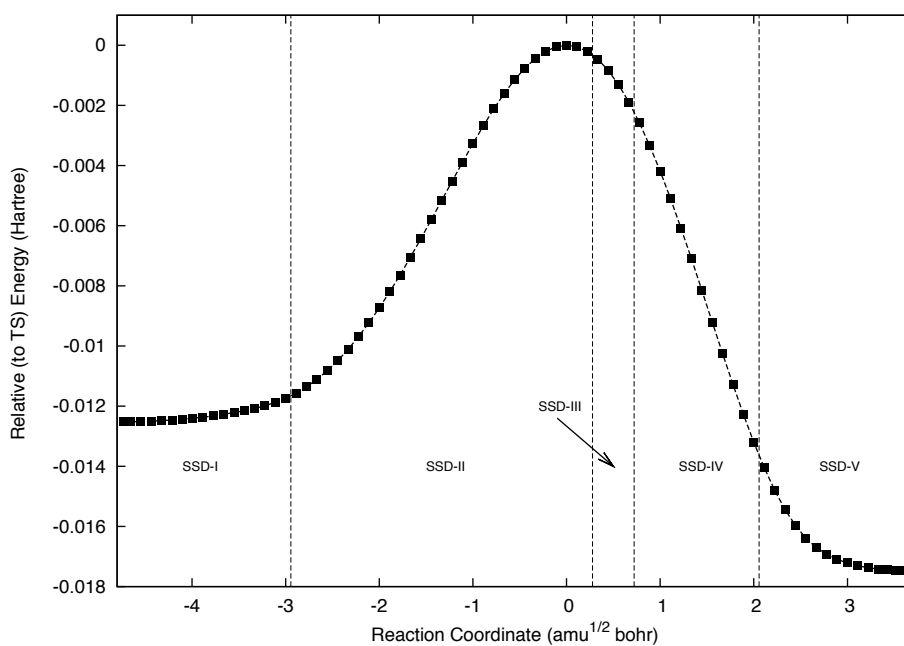


Scheme 2. CHT (left) isomerization to NCD (right)

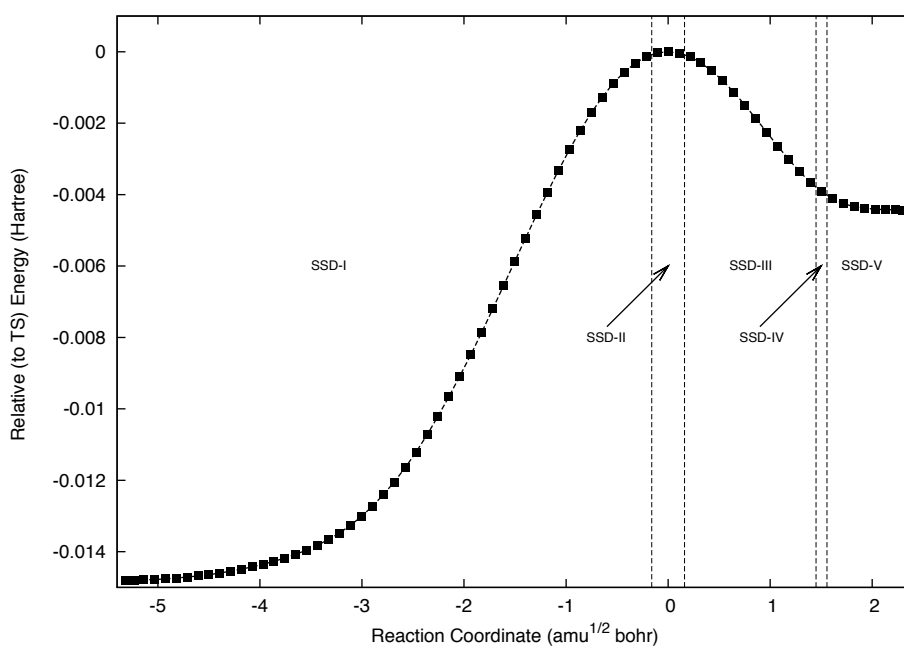
In general, the equilibrium lies on the CHT side, as a result of the strained cyclopropane ring present in the NCD tautomer. However, in 1965 the dicyano compound ($\text{R}_1=\text{R}_2=\text{CN}$) existing as stable NCD, was isolated by Ciganek.^[113] Since then, it has been established that electron-withdrawing substituents ($\text{R}=\text{CN}$, CO_2R ,

CHO, etc) tend to shift the equilibrium towards the NCD form, whereas π -electron donating groups (OR, NR₂, etc) tend to favor the CHT tautomer. Therefore, we have studied the two paradigmatic cases: the dicyano compound (**1**, R₁=R₂=CN) for NCD biased equilibrium and the dimethoxy compound (**2**, R₁=R₂=OCH₃) for CHT favored isomerism.

The calculations have been performed in these systems at B3LYP/6-31G(d) level of theory using Gaussian 09.^[110]As expected, we have found the NCD form of **1** to be more stable by 3.10 kcal/mol, and the CHT form of **2** to be more stable by 6.51 kcal/mol. The activation barriers have been calculated to be 10.96 and 9.29 kcal/mol, respectively. The corresponding energy profiles along the IRCs are reported in Figure 4, together with the five SSDs found in each case. Snapshots of the ELF basins for some selected points along the IRC representing the different SSDs are given in Figure 5, while the evolution of some basin populations along the IRC paths are reported in Figure 6.



(a)



(b)

Figure 4. IRC energy profile for the CHT (left side) to NCD (right side) isomerization of (a) **1**, and (b) **2**. The five domains of structural stability found in each case are marked.

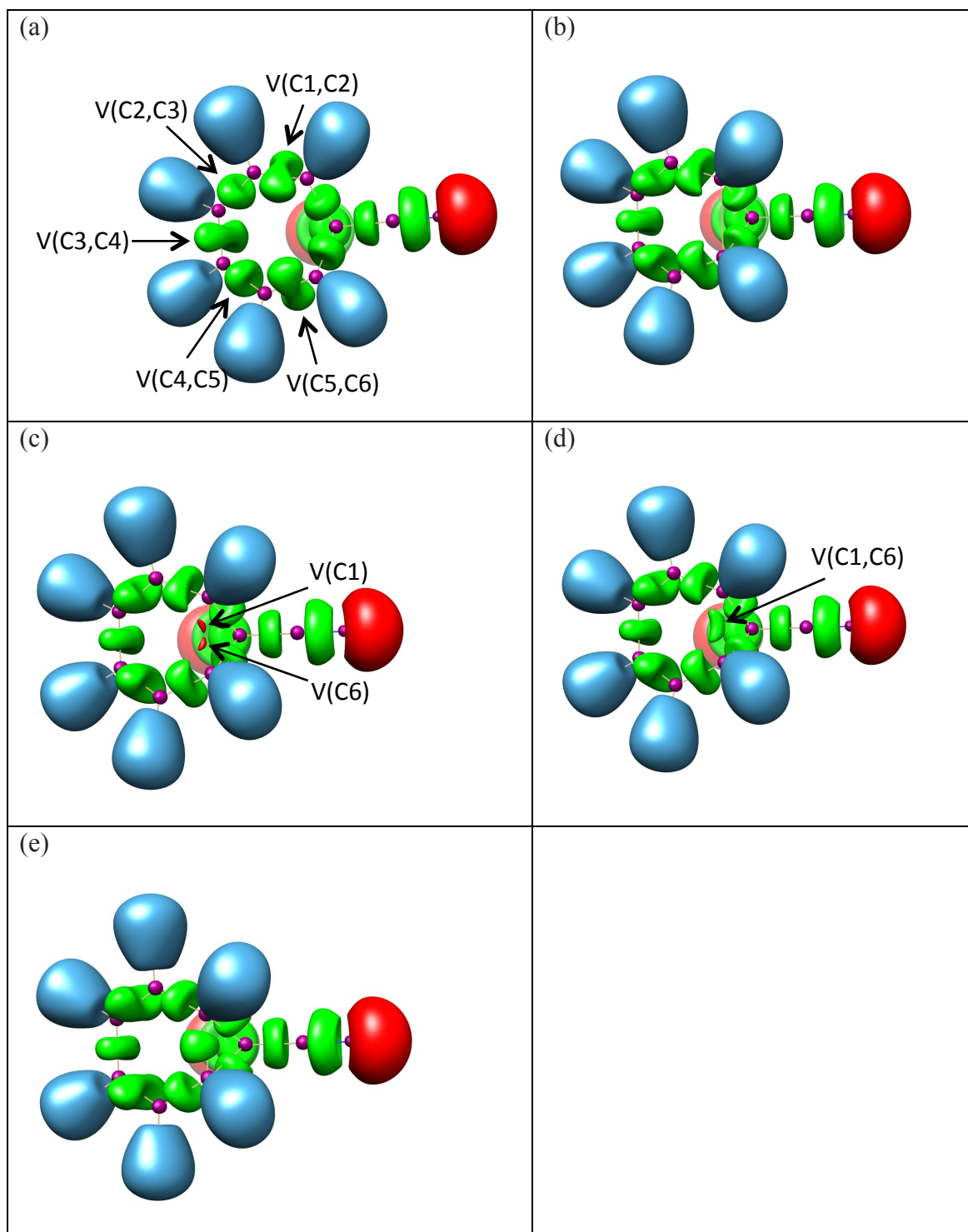


Figure 5a. Snapshots of the ELF localization domains ($\eta=0.753$ isosurface) for selected points along the IRC: (a) CHT tautomer of **1** (SSD-I), (b) TS belonging to SSD-II, (c) point at $s=0.556 \text{ amu}^{1/2}\text{bohr}$ belonging to SSD-III, (d) point at $s=0.778 \text{ amu}^{1/2}\text{bohr}$ belonging to SSD-IV, (e) NCD tautomer of **1**. The wireframe structure of the molecule is displayed for clarity. Names of some basins are included.

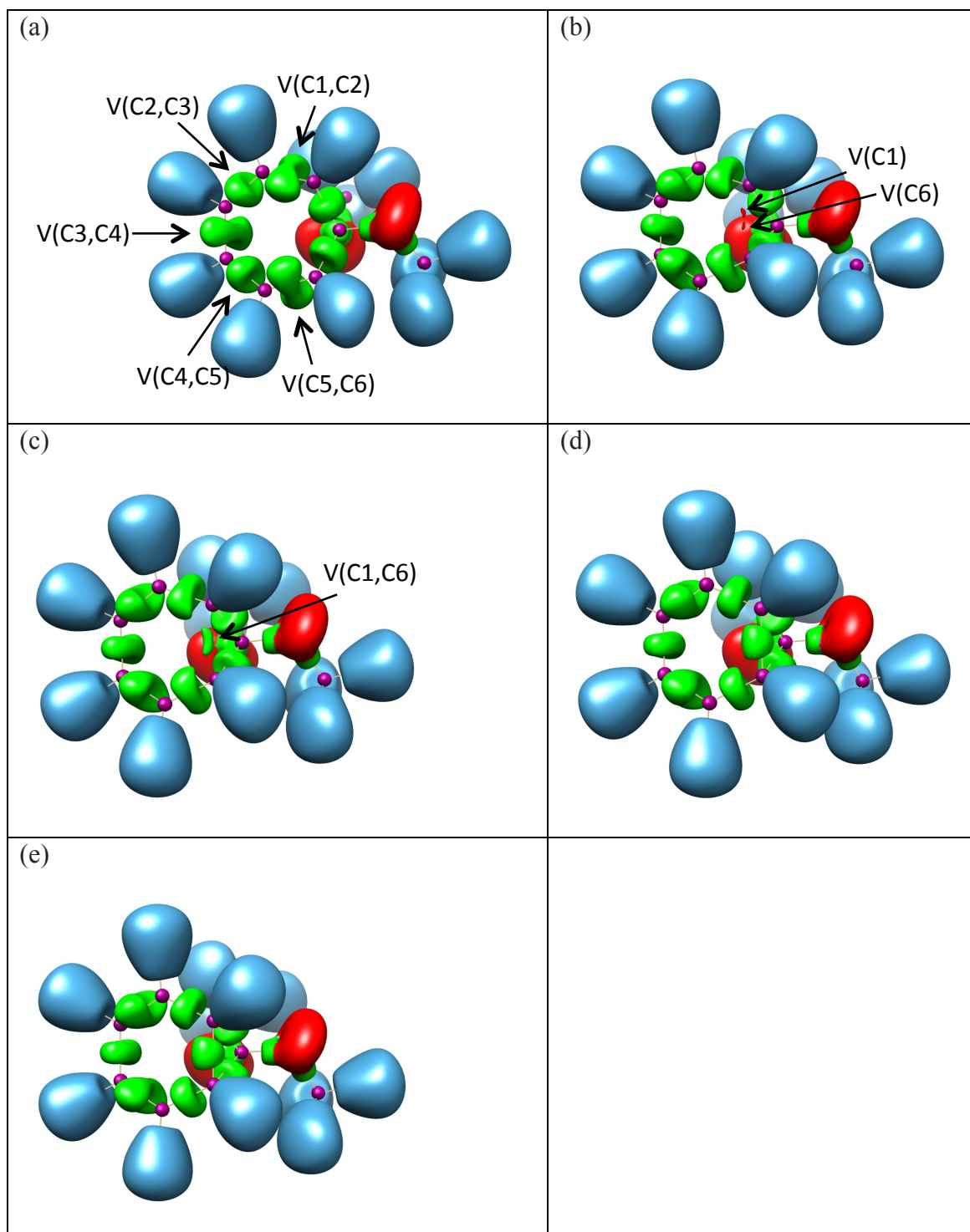
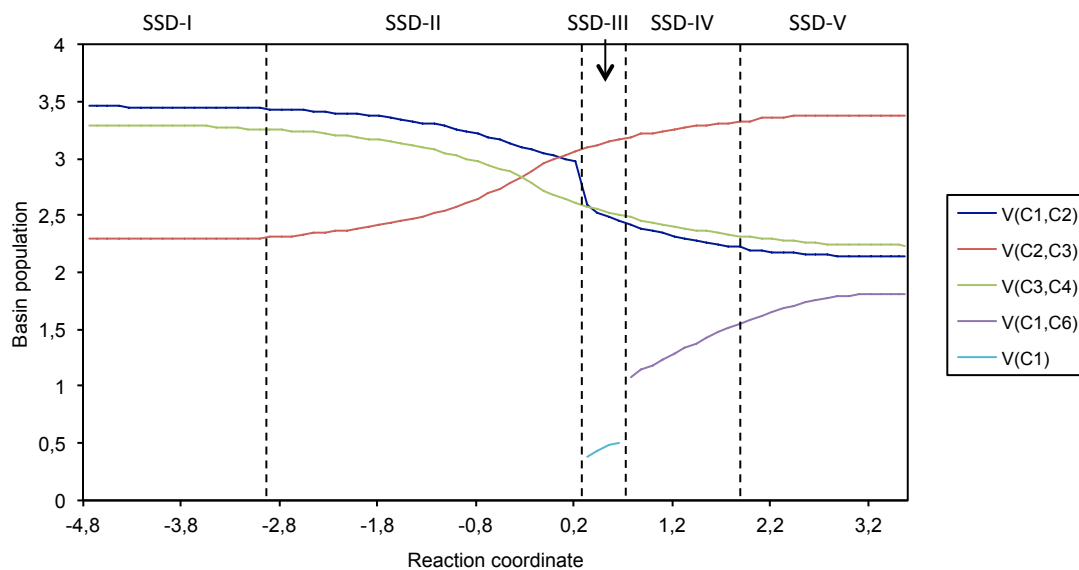
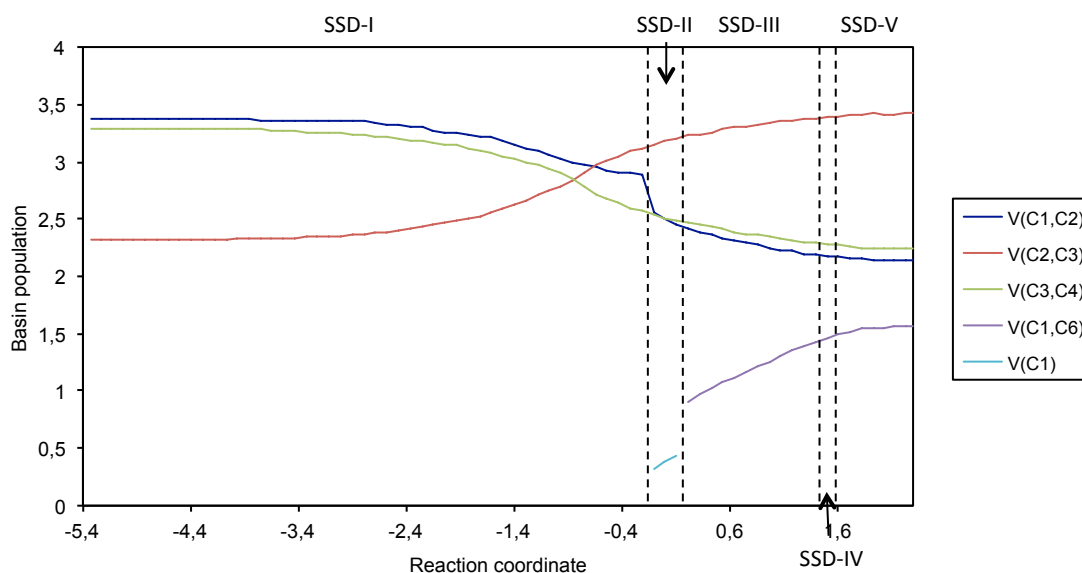


Figure 5b. Snapshots of the ELF localization domains ($\eta=0.741$ isosurface) for selected points along the IRC: (a) CHT tautomer of **2** (SSD-I), (b) TS belonging to SSD-II, (c) point at $s=0.215 \text{ amu}^{1/2}\text{bohr}$ belonging to SSD-III, (d) point at $s=1.503 \text{ amu}^{1/2}\text{bohr}$ belonging to SSD-IV, (e) NCD tautomer of **2**. Names of some basins are included



(a)

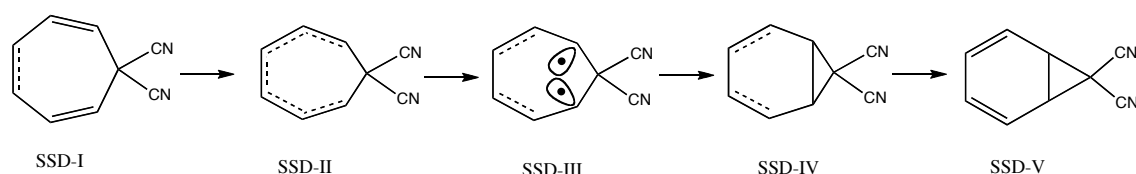


(b)

Figure 6. Population evolution of some basins along the IRC path for (a) **1**, and (b) **2**. The overall population of the two V(C1,C2) disynaptic basins is displayed for SSD-I, and the same happens with the overall population of the two V(C2,C3) disynaptic basins for SSD-V. Dashed lines separate the structural stability domains found, which are indicated.

At the CHT tautomer of **1**, left side of the energy profile in Figure 4a, 36 basins can be found, corresponding to 11 core basins, 6 hydrogenated basins, 2 monosynaptic basins corresponding to the lone pairs on the N atoms and a total of 17 disynaptic basins

accounting for the C-C and C-N bonds. It should be noted that the number of bonds in the classical Lewis representation (excluding the C-H bonds) of the molecule is 18 (six single bonds, three double bonds and two triple bonds). Conversely, the description of the ELF for the formal double C3=C4 bond is not reflected by a pair of disynaptic V(C3,C4) basins, as sometimes observed,^[64] but only single V(C3,C4) disynaptic basins were found with a population of 3.29e. This can be better observed with the help of Scheme 3, also depicted from the perspective of the ELF analysis as explained before.



Scheme 3. Representation of the CHT-NCD isomerization of **1** from the ELF perspective.

From this point onwards, along SSD-I, minor changes in the number of basins describing the C-N interactions can be sensed, not related to the chemical process under study. The first sound catastrophe can be found at $s \approx -2.94 \text{ amu}^{1/2} \text{ bohr}$: the two V(C1,C2) disynaptic basins related to the C1-C2 double bond merge into a single disynaptic basin and the same happens with the two disynaptic basins related to the C5-C6 double bond by means of cusp type catastrophes. The SSD-II includes a huge number of points along the IRC, among them the TS, whose ELF localization domains are depicted in Figure 5a (b). As it can be seen, there is no evidence of disynaptic basin between C1 and C6, and hence there is not such interaction –from the ELF topological point of view- at TS, although the C1-C6 distance has considerably shortened with respect to the CHT tautomer.

The overall populations of the two V(C1,C2) and the two V(C5,C6) basins, which were conserved (*ca* 3.46e) along SSD-I, slightly diminish in the change to SSD-II and the population loss becomes significant for these basins as the reaction proceeds. In Figure 6(a) the population evolution of V(C1,C2) is depicted, together with the population evolution of V(C2,C3), V(C3,C4), V(C1,C6) and V(C1) basins. Due to the symmetry of the molecule, the basins V(C1,C2) and V(C5,C6) behave in the same way and only the overall population of the V(C1,C2) basins is represented in Figure 6(a).

This is also the case of the basins $V(C2,C3)$ and $V(C4,C5)$, and of the basins $V(C1)$ and $V(C6)$.

Along SSD-II the population of the $V(C1,C2)$ basin (and $V(C5,C6)$, as explained) diminishes from 3.43 to 2.98e. The population of $V(C3,C4)$ also diminishes from 3.26e to 2.61e, while the population of $V(C2,C3)$ (and $V(C4,C5)$, of course) increases from 2.31 to 3.06e. This reflects the gradual loss of the double bond character of C1-C2, C5-C6 and C3-C4 as the reaction proceeds. This domain is the largest along the IRC and it is important to note that the TS is only one point in this region.

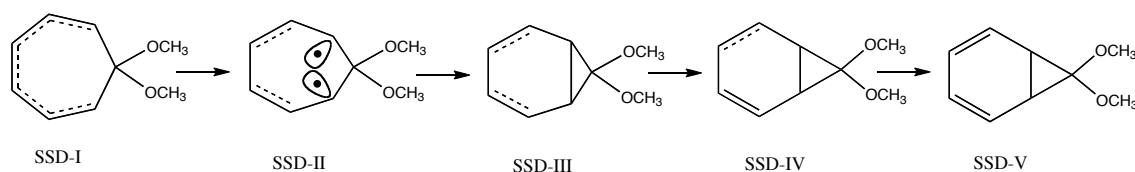
Once the TS has been reached and left behind, at $s \approx 0.278 \text{ amu}^{1/2} \text{ bohr}$, the second catastrophe is found. At this point, two new monosynaptic basins appear between C1 and C6 by means of fold type catastrophes, as it can be seen in Figure 5a(c) and in Scheme 3. The SSD-III is very short and at $s \approx 0.722 \text{ amu}^{1/2} \text{ bohr}$ these two monosynaptic basins merge into the disynaptic $V(C1,C6)$ basin accounting for the closing of the cyclopropane ring by means of a cusp type catastrophe. Finally, at $s \approx 2.056 \text{ amu}^{1/2} \text{ bohr}$, the last domain, SSD-V, is found characterized by the splitting of the $V(C2-C3)$ and $V(C4-C5)$ disynaptic basins into two disynaptic basins each, accounting for the double bonds formation.

Figure 6(a) shows that the population of the monosynaptic basins $V(C1)$ and $V(C6)$ comes mainly from the disynaptic $V(C1,C2)$ and $V(C5,C6)$. In the turning point between SSD-II and SSD-III, the population of these disynaptic basins goes down by 0.4e each, in correspondence with the population of the monosynaptic basins. Along SSD-III the population of the monosynaptic basins continues increasing and the population of the disynaptic basins decreasing accordingly. On the other hand, the population of $V(C3,C4)$ becomes larger than the population of $V(C1,C2)$ at the beginning of SSD-III, and from there on, its evolution parallels the evolution of $V(C1,C2)$ with populations always slightly larger. The $V(C1)$ and $V(C6)$ monosynaptic basins disappear in the turning point between SSD-III and SSD-IV, replaced by the disynaptic $V(C1,C6)$ basin, whose population continuously increases from 1.08e at the beginning of SSD-IV, to 1.8e at the end of SSD-V. Along these two domains, the population of $V(C2,C3)$ and $V(C4,C5)$ increases to reach 3.38e, while the populations of $V(C1,C2)$, $V(C3,C4)$ and $V(C5,C6)$ diminishes to 2.14, 2.23, and 2.14e, respectively.

Therefore, from a topological point of view the reaction as a whole can be described as an electron density transfer from basins $V(C1,C2)$, $V(C3,C4)$ and $V(C5,C6)$ to basins $V(C2,C3)$, $V(C4,C5)$ and $V(C1,C6)$, in agreement with the classical

electron-arrow moving scheme. However, the topological study by means of the BET approach offers a detailed description of what is going on as the reaction proceeds, revealing unknown aspects of the electronic rearrangements.

As for the dimethoxy derivative, at the CHT tautomer of **2**, left side of the energy profile in Figure 4b, 38 basins can be found, corresponding to 11 core basins, 12 hydrogenated basins, 4 monosynaptic basins corresponding to the lone pairs on the O atoms and a total of 11 disynaptic basins accounting for the C-C and C-O bonds. In this case, the number of bonds in the classical Lewis representation of the molecule (again excluding the C-H's) is 14 (eight single bonds and three double bonds). The ELF topological description found differs from this view in that the C1-C2, C3-C4 and C5-C6 interactions are described by *single* disynaptic basins with populations of 3.38, 3.29, and 3.39e, respectively, instead of by *double* disynaptic basins. These populations go down to 2.89, 2.57 and 2.87e, respectively, along SSD-I, while the populations of V(C2,C3) and V(C4,C5) increase from 2.32 each to 3.12 and 3.13e, respectively. Hence, along SSD-I there is a redistribution of population within the cycle. This can be better observed with the help of Scheme 4. In contrast to the previous example, the SSD-I is the largest domain along the IRC with the largest contribution to activation energy of the process. A comparison of Schemes 3 and 4 renders similar ELF representation, SSD-II and SSD-I for the step controlling the energy cost of CHT-NCD isomerization of **1** and **2**, respectively.



Scheme 4. Representation of the CHT-NCD isomerization of **2** from the ELF perspective.

Very close to the TS, at $s \approx -0.161 \text{ amu}^{1/2} \text{ bohr}$, the first turning point has been found with the appearance of two monosynaptic basins between C1 and C6 by means of fold type catastrophes, as it can be seen in Figure 5b(b) and in Scheme 4. The SSD-II is also very short in this case and at $s \approx 0.161 \text{ amu}^{1/2} \text{ bohr}$ these two monosynaptic basins merge into the disynaptic V(C1,C6) basin by means of a cusp type catastrophe accounting for the closing of the cyclopropane ring. Due to the non-symmetric character

of this molecule, the V(C4,C5) basin splits to reflect its double bond character at $s \approx 1.450 \text{ amu}^{1/2} \text{ bohr}$, while the V(C2,C3) basin splits at $s \approx 1.557 \text{ amu}^{1/2} \text{ bohr}$ where the last domain, SSD-V, is found.

As explained above, Figure 6(b) indicates that the population of the monosynaptic basins V(C1) and V(C6) mainly comes from the disynaptic V(C1,C2) and V(C5,C6) basins. In the turning point between SSD-I and SSD-II the population of these disynaptic basins goes down by $ca 0.3e$ each, in correspondence with the population of the monosynaptic basins. Along SSD-II, the population of the monosynaptic basins continues to increase and the population of the disynaptic basins decreases accordingly. On the other hand, the population of V(C3,C4) becomes larger than the population of V(C1,C2) at the beginning of SSD-II, and from there on, its evolution parallels the evolution of V(C1,C2) with populations always slightly larger. The V(C1) and V(C6) monosynaptic basins disappear in the turning point between SSD-II and SSD-III, replaced by the disynaptic V(C1,C6) basin, whose population continuously increases from 0.9e, at the beginning of SSD-III, to 1.56e at the end of SSD-V. Along these three domains, the population of V(C2,C3) and V(C4,C5) increases to reach 3.42e, while the populations of V(C1,C2), V(C3,C4) and V(C5,C6) diminish to 2.14, 2.24 and 2.13e, respectively.

As it can be seen, the description of the CHT-NCD isomerization processes from a topological point of view is very similar for **1** and **2**. Two main differences can be mentioned have been found: on one hand, at the CHT side for **2**, no splitting of the double bonds has been found, whereas for **1** two of the three double bonds are described with two disynaptic basins. On the other hand, and perhaps more importantly, a significant difference in the population of the V(C1,C6) basin has been noticed at the NCD side: for **1** the population is 1.8e, while for **2** it is only 1.56e. This can be related to the lower stability of the NCD form of **2**, due to the weakness of this bond. This hypothesis needs to be tested with more cases and work is being conducted to address this issue.

Conclusions and Outlook

One of the aims of chemistry, as a basic science, is to study and explain the structure of the matter and its transformations, i.e. chemical structure and reactivity. By explain it is meant that science has to explain how and why a given phenomenon occurs

in given circumstances and understanding the basic science behind this has been one of the main challenges of theoretical and computational chemistry.

As remarked by Wang^[114]: “Christopher Ingold, a major early contributor to mechanistic organic chemistry, astutely foreshadowed the future development of organic synthesis in the following statement:^[115,116] *“The new work made it inescapably clear that the old order in organic chemistry was changing, the art of the subject diminishing, its science increasing: no longer could one just mix things; sophistication in physical chemistry was the base from which all chemists, including the organic chemist, must start.”* The current state of the understanding of chemical reactivity is comparable to that of organic synthesis a century ago. The chemical interpretation of the reaction mechanism has undergone a substantial evolution since the earliest successes of the nowadays well established potential energy surface. However, apprehending the nature of chemical mechanisms, where classical concepts are inadequate, demands proper quantum physical frameworks. A reaction mechanism is usually studied by finding the reactants, products, intermediates and transition states on potential energy surface. The purpose is not to justify or invalidate the models based on the analysis of the energetic, geometric and electronic aspects derived from the characterization of potential energy surface but to rather establish correspondences between the assumed concepts and quantum mechanics.

The combination of the ELF and Thom’s catastrophe theory has been consolidated as a powerful tool to analyze the course of a given chemical rearrangement and allows us to identify how electronic flow in a molecule occurs as a function of reaction progress, which constitutes the motivation of the present work. In the present study, we have used the ELF and CT to analyze and monitor the progress of chemical events, i.e., bond breaking/forming process, lone pair rearrangements, etc. along a given reaction mechanism. Taking into account this theoretical background, the purpose of this paper has been to study the evolution of atomic interactions by means of a QTC description. QTC analysis proves relevant to a surprisingly wide range of modern physical chemistry, with the latest applications affording fresh and richer insights, more correct descriptions of mechanism and the revelation of entirely new phenomena.

Two chemical rearrangements have been here studied: the simple isomerization of carbene $C(BH)_2$ and a complex process corresponding to the thermal norcaradiene-cycloheptatriene isomerization of both dicyano and dimethoxy compounds. In particular, for these chemical rearrangements, we can answer the following questions:

(i) how can the electronic reorganization proceed along the reaction path? (ii) Are they flowing synchronously? (iii) In which direction? (iv) When and how do the bond formation/breaking processes take place along the reaction path?(v) Do the bond formation/breaking processes take place at the TS? (vi) When do the electron pair rearrangements take place along the reaction pathway? For the carbene isomerization, we also respond to: (vii) How can the electron flow be related to the electron-pair rearrangements? (viii) Whose are the electron pairs involved in the electronic reorganization? While for the norcaradiene-cycloheptatriene isomerization, the answered questions are: (ix) how and to what extent substituent effects modify the reaction mechanism? And (x) Is it possible to understand and rationalize the role of substituent effects? These questions are addressed here by employing QTC to characterize the reaction mechanism and follow their density redistribution along the reaction pathway. This goal has required extension of the relationships between the traditional chemical concepts and the quantum mechanical ones and it is in agreement with physical laws and quantum theoretical insights. So, it can be considered as an appropriate tool to tackle chemical reactivity with a wide range of possible applications and the universal behaviour that it predicts. Further development and exploitation of the present strategy have the potential to deliver the reaction mechanism unique semi-quantitative insight into the origins of catalytic processes.

Acknowledgements

The authors are grateful to Generalitat Valenciana for *Prometeo/2009/053* project, Ministerio de Economía y Competitividad (Spain) for project CTQ-2012-36253-C03-02, and Universitat Jaume I-Fundació Bancaixa, for projects P1·1B2010-10 and P1·1B2013-40. The authors are also grateful to the Servei d'Informàtica, Universitat Jaume I for generous allocation of computer time.

References

- [1] J. K. Gilbert, C. J. Boulter, R. Elmer, *Developing Models in Science Education*; Gilbert, J. K.; Boulter, C. J., Eds.; Kluwer Academic Publisher: Dordrecht, 2000, p 3.
- [2] N. M. Gericke, M. Hagberg, *Science & Education* **2007**, *16*, 849.
- [3] A. Bergqvist, M. Drechsler, O. De Jong, S.-N. C. Rundgren, *Chem. Educ. Res. Pract.* **2013**, *14*, 589.
- [4] H. Jacobsen, *J. Comput. Chem.* **2008**, *30*, 1093.
- [5] H. Jacobsen, *Dalton Trans.* **2010**, *39*, 5426.
- [6] J. F. Gonthier, S. N. Steinmann, M. D. Wodrich, C. Corminboeuf, *Chem. Soc. Rev.* **2012**, *41*, 4671.
- [7] S. Álvarez, R. Hoffmann, C. Mealli, *Chem. Eur. J.* **2009**, *15*, 8358.
- [8] P. Ball, *Nature* **2011**, *469*, 26.
- [9] G. Frenking, A. Krapp, *J. Comput. Chem.* **2007**, *28*, 15.
- [10] S. Shaik, H. S. Rzepa, R. Hoffmann, *Angew. Chem. Int. Edit.* **2013**, *52*, 3020.
- [11] G. Frenking, M. Hermann, *Angew. Chem. Int. Edit.* **2013**, *52*, 5922.
- [12] R. G. Parr, P. W. Ayers, R. F. Nalewajski, *J. Phys. Chem. A* **2005**, *109*, 3957.
- [13] H. Jacobsen, *Phys. Chem. Chem. Phys.* **2013**, *15*, 5057.
- [14] G. B. Bacskay, S. Nordholm, *J. Phys. Chem. A* **2013**, *117*, 7946.
- [15] C. Esterhuysen, G. Frenking, *Theor. Chem. Acc.* **2005**, *113*, 294.
- [16] V. Tognetti, L. Joubert, C. Adamo, *J. Chem. Phys.* **2010**, *132*, 211101.
- [17] R. B. Grossman, *The art of writing reasonable organic reaction mechanisms*; Springer-Verlag: New York, 2003.
- [18] J. A. Berson, *Rearrangements in Ground and Excited States*; de Mayo, P., Ed.; Academic Press: New York, 1980, p 311.
- [19] T. H. Lowry, K. S. Richardson, *Mechanism and Theory in Organic Chemistry*; Harper & Row: New York, 1987.
- [20] J. J. Gajewski, *Hydrocarbon Thermal Isomerizations*; Elsevier: Amsterdam, 2004.
- [21] E. V. Anslyn, D. A. Dougherty, *Modern Physical Organic Chemistry*; University Science Books: Sausalito, CA, 2006.
- [22] M. B. Smith, *March's Advanced Organic Chemistry: Reactions, Mechanisms, and Structure*; Wiley: Hoboken, 2013.
- [23] K. P. C. Vollhardt, N. E. Schore, *Organic Chemistry: Structure and Function*; W. H. Freeman: New York, 2007.
- [24] R. G. Wilkins, *Kinetics and Mechanism of Reactions of Transition Metal Complexes*; Wiley-VCH Verlag: Weinheim, Germany, 2003.
- [25] R. B. Jordan, *Reaction Mechanisms of Inorganic and Organometallic Systems*; Oxford University Press: Oxford, 2007.
- [26] C. K. Mathews, K. E. van Holde, K. G. Ahern, *Biochemistry*; Prentice-Hall: Upper Saddle River, NJ, 1999.
- [27] D. L. Nelson, M. M. Cox, *Lehninger Principles of Biochemistry*; W. H. Freeman and Company: New York, 2008.
- [28] D. Himmel, I. Krossing, A. Schnepf, *Angew. Chem. Int. Edit.* **2013**.
- [29] S. Alvarez, *Angew. Chem. Int. Edit.* **2012**, *51*, 590.
- [30] M. Born, K. Huang, *Dynamical Theory of Crystal Lattices*; Oxford University Press: Oxford, 1998.
- [31] M. Born, J. R. Oppenheimer, *Ann. Phys.* **1927**, *84*, 457.

- [32] J. C. Slater, *Proc. Natl. Acad. Sci.* **1927**, *13*, 423.
- [33] D. Wales, *Energy Landscapes: Applications to Clusters, Biomolecules and Glasses*; Cambridge University Press: Cambridge, 2003.
- [34] C. A. Coulson, *The Spirit of Applied Mathematics*; Clarendon Press, 1953, p 20.
- [35] G. N. Lewis, *J. Am. Chem. Soc.* **1916**, *38*, 762.
- [36] S. Shaik, *J. Comput. Chem.* **2006**, *28*, 51.
- [37] C. Aslangul, R. Constanciél, R. Daudel, P. Kottis, *Advances in Quantum Chemistry*; Lowdin, P. O., Ed.; Academic Press: New York, 1972, p 94.
- [38] A. J. Cohen, P. Mori-Sánchez, W. Yang, *Science* **2008**, *321*, 792.
- [39] W. Kohn, L. J. Sham, *Phys. Rev.* **1965**, *140*, A1133.
- [40] R. G. Parr, W. Yang, *Density Functional Theory of Atoms and Molecules*; Oxford University Press: New York, 1989.
- [41] P. C. Hohenberg, W. Kohn, *Phys. Rev.* **1964**, *136*, B864.
- [42] R. F. W. Bader, G. A. Jones, *J. Chem. Phys.* **1963**, *38*, 2791.
- [43] P. O. Lowdin, *Adv. Chem. Phys.* **1959**, *2*, 207.
- [44] T. S. Koritsanszky, P. Coppens, *Chem. Rev.* **2001**, *101*, 1583.
- [45] P. Coppens, *Phys. Scr.* **2013**, *87*, 048104.
- [46] R. F. W. Bader, *Foundations of Chemistry* **2011**, *13*, 11.
- [47] P. A. M. Dirac, *The Principles of Quantum Mechanics*; Oxford University Press: Oxford, 1981.
- [48] R. F. W. Bader, *Atoms in Molecules: a Quantum Theory*; Oxford University Press: Oxford, 1990.
- [49] P. L. Popelier, *Atoms in Molecules: an Introduction*; Pearson Education: Harlow, 2000.
- [50] C. F. Matta, J. B. Russel, A. Becke, *The Quantum Theory of Atoms in Molecules: From Solid State to DNA and Drug Design*; Wiley-VCH: Weinheim, 2007.
- [51] R. F. W. Bader, *Chem. Rev.* **1991**, *91*, 893.
- [52] R. F. W. Bader, *Theor. Chem. Acc.* **2001**, *105*, 276.
- [53] P. L. Popelier, *Coord. Chem. Rev.* **2000**, *197*, 169.
- [54] F. Cortés-Guzmán, R. F. W. Bader, *Coord. Chem. Rev.* **2005**, *249*, 633.
- [55] G. Merino, A. Vela, T. Heine, *Chem. Rev.* **2005**, *105*, 3812.
- [56] R. F. W. Bader, *J. Phys. Chem. A* **1998**, *102*, 7314.
- [57] R. Bianchi, G. Gervasio, D. Marabello, *Inorg. Chem.* **2000**, *39*, 2360.
- [58] C. F. Matta, *Hydrogen Bonding—New Insights*; Grabowski, S. J., Ed.; Springer: Dordrecht, 2006, p 337.
- [59] R. Abraham, C. D. Shaw. *Dynamics: the Geometry of Behavior*; Addison Wesley: Redwood City, 1992.
- [60] R. Abraham, J. E. Marsden. *Foundations of Mechanics*; Addison Wesley: Redwood City, 1994.
- [61] DFG priority program 1178: "Experimental Electron Density as Key to Understanding Chemical Interactions". <http://onlinelibrary.wiley.com/doi/10.1002/zaac.v639.11/issuetoc> in *Journal of Inorganic and General Chemistry*, 2013, p 1893.
- [62] A. D. Becke, K. E. Edgecombe, *J. Chem. Phys.* **1990**, *92*, 5397.
- [63] B. Silvi, A. Savin, *Nature* **1994**, *371*, 683.
- [64] A. Savin, B. Silvi, F. Colonna, *Can. J. Chem.* **1996**, *74*, 1088.
- [65] R. Nesper, *Angew. Chem. Int. Edit.* **1991**, *30*, 789.
- [66] A. Savin, R. Nesper, S. Wengert, T. F. Fässler, *Angew. Chem. Int. Edit.* **1997**, *36*, 1808.
- [67] D. B. Chesnut, *J. Phys. Chem. A* **2000**, *104*, 11644.

- [68] A. Kumar, S. R. Gadre, N. Mohan, C. H. Suresh, *J. Phys. Chem. A* **2014**, *118*, 526.
- [69] P. L. A. Popelier, *Structure and Bonding: Intermolecular Forces and Clusters I*; Wales, D. J., Ed.; Springer: Heidelberg, 2005.
- [70] P. L. A. Popelier, P. J. Smith, *Specialist Periodical Reports Chemical Modelling: Applications and Theory*; Hinchliffe, A., Ed.; The Royal Society of Chemistry: Cambridge, 2002, p 391.
- [71] P. L. A. Popelier, F. M. Aicken, S. E. O'Brien, *Specialist Periodical Reports Chemical Modelling: Applications and Theory*; Hinchliffe, A., Ed.; The Royal Society of Chemistry: Cambridge, 2000, p 143.
- [72] C. Gatti, *The Quantum Theory of Atoms in Molecules: from Solid State to DNA and Drug Design*; Boyd, R. J.; Matta, C. F., Eds.; Wiley-VCH: Weinheim, 2007, p 165.
- [73] A. M. Simas, V. H. Smith Jr., A. J. Thakkar, *Int. J. Quantum Chem.* **1984**, *26*, 385.
- [74] R. F. W. Bader, G. L. Heard, *J. Chem. Phys.* **1999**, *111*, 8789.
- [75] Y. Tal, R. F. W. Bader, J. Erkkü, *Phys. Rev. A* **1980**, *21*, 1.
- [76] T. A. Keith, R. F. W. Bader, Y. Aray, *Int. J. Quantum Chem.* **1996**, *57*, 183.
- [77] R. F. W. Bader, P. J. MacDougall, C. D. H. Lau, *J. Am. Chem. Soc.* **1984**, *106*, 1594.
- [78] R. F. W. Bader, R. J. Gillespie, P. J. MacDougall, *J. Am. Chem. Soc.* **1988**, *110*, 7329.
- [79] P. Balanarayan, R. Kavathekar, S. R. Gadre, *J. Phys. Chem. A* **2007**, *111*, 2733.
- [80] P. G. Mezey, *Theor. Chim. Acta* **1981**, *58*, 309.
- [81] P. G. Mezey, *Potential Energy Hypersurfaces*; Elsevier: Amsterdam, 1987.
- [82] R. F. W. Bader, *Phys. Rev. B* **1994**, *49*, 13348.
- [83] R. Thom, *Nature* **1977**, *270*, 658.
- [84] R. F. W. Bader, Y. Tal, S. G. Anderson, T. T. Nguyen-Dang, *Isr. J. Chem.* **1980**, *19*, 8.
- [85] T. T. Nguyen-Dang, R. F. W. Bader, *Physica A: Statistical Mechanics and its Applications* **1982**, *114*, 68.
- [86] R. F. W. Bader, T. T. Nguyen-Dang, Y. Tal, *Rep. Prog. Phys.* **1981**, *44*, 893.
- [87] R. Thom. *Structural Stability and Morphogenesis*; W. A. Benjamin Inc.: Redding, 1976.
- [88] T. Poston, I. Stewart. *Catastrophe Theory and its Applications*; Dover Publications: Pitman, 1978.
- [89] X. Krokidis, S. Noury, B. Silvi, *J. Phys. Chem. A* **1997**, *101*, 7277.
- [90] A. Savin, O. Jepsen, J. Flad, O. K. Andersen, H. Preuss, H. G. v. Schnering, *Angew. Chem. Int. Edit.* **1992**, *31*, 187.
- [91] X. Krokidis, R. Vuilleumier, D. Borgis, B. Silvi, *Mol. Phys.* **1999**, *96*, 265.
- [92] B. Silvi, *J. Mol. Struct. Theochem* **2002**, *614*, 3.
- [93] S. Berski, J. Andrés, B. Silvi, L. R. Domingo, *J. Phys. Chem. A* **2006**, *110*, 13939.
- [94] S. Noury, X. Krokidis, F. Fuster, B. Silvi, *Computers & Chemistry* **1999**, *23*, 597.
- [95] K. Fukui, *J. Phys. Chem.* **1970**, *74*, 4161.
- [96] K. Fukui, *Acc. Chem. Res.* **1981**, *14*, 363.
- [97] Y. Zeng, L. Meng, X. Li, S. Zheng, *J. Phys. Chem. A* **2007**, *111*, 9093.
- [98] X. Li, H. Fan, L. Meng, Y. Zeng, S. Zheng, *J. Phys. Chem. A* **2007**, *111*, 2343.
- [99] Y. Zeng, S. Zheng, L. Meng, *J. Phys. Chem. A* **2004**, *108*, 10527.
- [100] Y. Zeng, S. Zheng, L. Meng, *Inorg. Chem.* **2004**, *43*, 5311.

- [101] N. O. Malcom, P. L. A. Popelier, *J. Phys. Chem. A* **2001**, *105*, 7638.
- [102] V. Polo, J. Andrés, R. Castillo, S. Berski, B. Silvi, *Chem. Eur. J.* **2004**, *10*, 5165.
- [103] P. González-Navarrete, J. Andrés, S. Berski, *J. Phys. Chem. Lett.* **2012**, *3*, 2500.
- [104] P. González-Navarrete, L. R. Domingo, J. Andrés, S. Berski, B. Silvi, *J. Comput. Chem.* **2012**, *33*, 2400.
- [105] M. E. Alikhani, M. d. C. Michelini, N. Russo, B. Silvi, *J. Phys. Chem. A* **2008**, *112*, 12966.
- [106] A. S. Nizovtsev, S. G. Kozlova, *J. Phys. Chem. A* **2013**, *117*, 481.
- [107] A. S. Nizovtsev, *J. Comput. Chem. A* **2013**, *34*, 1917.
- [108] C. H. Suresh, N. Koga, S. R. Gadre, *J. Org. Chem.* **2001**, *66*, 6883.
- [109] S. R. Barua, W. D. Allen, E. Kraka, P. Jerabek, R. Sure, G. Frenking, *Chem. Eur. J.* **2013**, *19*, 15941.
- [110] Gaussian 09, Revision B.01, M. J. Frisch, G. W. Trucks, H. B. Schlegel, G. E. Scuseria, M. A. Robb, J. R. Cheeseman, G. Scalmani, V. Barone, B. Mennucci, G. A. Petersson, H. Nakatsuji, M. Caricato, X. Li, H. P. Hratchian, A. F. Izmaylov, J. Bloino, G. Zheng, J. L. Sonnenberg, M. Hada, M. Ehara, K. Toyota, R. Fukuda, J. Hasegawa, M. Ishida, T. Nakajima, Y. Honda, O. Kitao, H. Nakai, T. Vreven, J. A. Montgomery, Jr., J. E. Peralta, F. Ogliaro, M. Bearpark, J. J. Heyd, E. Brothers, K. N. Kudin, V. N. Staroverov, R. Kobayashi, J. Normand, K. Raghavachari, A. Rendell, J. C. Burant, S. S. Iyengar, J. Tomasi, M. Cossi, N. Rega, J. M. Millam, M. Klene, J. E. Knox, J. B. Cross, V. Bakken, C. Adamo, J. Jaramillo, R. Gomperts, R. E. Stratmann, O. Yazyev, A. J. Austin, R. Cammi, C. Pomelli, J. W. Ochterski, R. L. Martin, K. Morokuma, V. G. Zakrzewski, G. A. Voth, P. Salvador, J. J. Dannenberg, S. Dapprich, A. D. Daniels, Ö. Farkas, J. B. Foresman, J. V. Ortiz, J. Cioslowski, and D. J. Fox, Gaussian, Inc., Wallingford CT, 2009.
- [111] O. A. McNamara, A. R. Maguire, *Tetrahedron* **2011**, *67*, 9.
- [112] R. Beniazza, V. Desvergnés, E. Girard, B. Kauffmann, M. Berlande, Y. Landais, *Chem. Eur. J.* **2012**, *18*, 11976.
- [113] E. Ciganek, *J. Am. Chem. Soc.* **1965**, *87*, 652.
- [114] F. Wang, V. N. Richards, S. P. Shields, W. E. Buhro, *Chem. Mater* **2013**, *ASAP*.
- [115] C. W. Shoppee, *Biogr. Mem. Fell. R. Soc.* **1972**, *18*, 349.
- [116] D. H. R. Barton, *Bull. Hist. Chem.* **1996**, *19*, 43.

GRAPHICAL ABSTRACT

AUTHOR NAMES

Juan Andrés*, Patricio González-Navarrete, and Vicent Sixte Safont

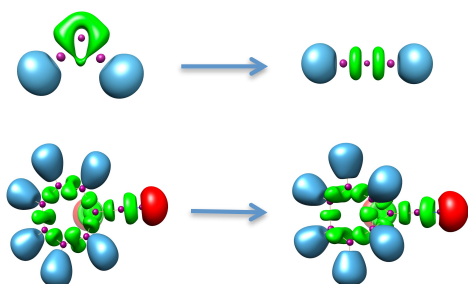
TITLE

Unraveling Reaction Mechanisms by means of Quantum Chemical Topology Analysis

TEXT

A review is offered on the use of the Bonding Evolution Theory to describe the electronic rearrangements within chemical processes. To illustrate its applicability, the isomerization of $C(BH)_2$ carbene (up), and thermal cycloheptatriene-norcaradiene isomerizations (down) have been studied here.

GRAPHICAL ABSTRACT FIGURE



AUTHOR BIOGRAPHIES



Juan Andrés is Full Professor of Physical Chemistry at the Universitat Jaume I, and Director of Theoretical and Computational Chemistry Group and completed his Ph.D. degree in Physical Chemistry at Universitat of Valencia, Spain, under the supervision of Prof. E. Silla in 1984. He undertook postdoctoral studies at Uppsala Universitet, in Sweden, with Prof. Orlando Tapia. Prof. Andrés was invited Professor at the Université Pierre et Marie Curie (Paris, France) working with Prof. B. Silvi; and at National Institute of Science and Technology of Materials in Nanotechnology, (Sao Carlos, Brazil) directed by Prof. E. Longo. His research interest covers a wide range of fields from structure and chemical reactivity, nanoscience and nanotechnology, materials science and catalysis.



Patricio González Navarrete studied chemistry at the Universidad de Chile. He received his Ph.D. from the Universitat Jaume I and the Université Pierre et Marie Curie in 2011. His research focuses on the description of chemical reactivity based on the topological analysis of the electronic localization function, and the study of chemical reactions which involve two state reactivity mechanisms. Since February 2014, P.G-N is an Alexander von Humboldt Postdoctoral fellow at the Technische Universität Berlin.



Vicent S. Safont is Full Professor of Physical Chemistry at the Universitat Jaume I. He received his Ph.D. in Physical Chemistry at the same University, under the supervision of Prof. J. Andrés in 1994. His research is in the field of theoretical and computational chemistry, particularly in theoretical studies of reaction mechanisms in organic and inorganic chemistry, as well as in biochemical and enzymatic processes.